J Radioanal Nucl Chem (2015) 303:2173–2183
DOI 10.1007/s10967-014-3755-0

Comparison of adsorption behavior of Th(IV) and U(VI) on mixed-ligands impregnated resin containing antraquinones with that conventional one

Mohammad Saeid Hosseini · Fatemeh Abedi

Received: 1 August 2014 / Published online: 1 November 2014

Abstract Mutual separation of Th(IV) and U(VI) ions is very important in industry. Two newly solvent impregnated resins (SIRs) were prepared for this investigation. One of the SIRs contents 1,4-diaminoantraquinone (DAAQ) and the other one contains 1,4-dihydroxyantraquinone and DAAQ as 1:1 mixed-ligands. Comparison of adsorption behavior of Th(IV) and U(VI) on both types the SIRs were carried out using several models. The results showed that the adsorption behavior of the mixed-ligands SIR is methodically differs from the other one so that the successful separation of U(VI) from Th(IV) is feasible using the mixed-ligands SIR.

Keywords Solvent impregnated resin (SIR) · Th(IV) · U(VI) · 1,4-Diaminoantraquinone · 1,4- Dihydroxyantraquinone · Amberlite XAD-16

List of symbols

- A_T Temkin constant (mg L^{-1})
- b Langmuir constant related to the free energy of adsorption (L mg^{-1})
- B_T Temkin constant (L g^{-1})
- C_0 The initial metal ion concentration (mg L^{-1})
- C_e The equilibrium concentration of metal ion in the balk solution (mg L^{-1})
- I The intercept of intraparticle diffusion eq. related to boundary layer thickness
- K_F Frendlich constant indicative of the relative adsorption capacity of SIR ($mg^{1-(1/n)}$ $L^{1/n}$ g^{-1})
- k_1 Rate constant of pseudo-first-order adsorption (min^{-1})
- k_2 Rate constant of pseudo-second-order adsorption (g mg^{-1} min)
- k_i Rate constant of the intraparticle diffusion (mg g^{-1} $min^{-0.5}$)
- n Frendlich constant indicative of the intensity of the adsorption
- q_e The amount of metal ion adsorbed per unit weight of SIR at equilibrium (mg g^{-1})
- q_m The theoretical monolayer saturation capacity (mg g^{-1})
- q_t The amount of metal ion adsorbed per unit weight of SIR at time t (mg g^{-1})
- R_L Separation factor, also called equilibrium parameter
- T Temperature (K)
- t Contact time (min)
- α Elovich equation, the initial adsorption rate (mg g^{-1} min)
- β Elovich equation, the parameter related to the extent of surface coverage and activation energy for chemisorption b (g mg^{-1})

Introduction

Application of uranium and thorium has been extensively developed as nuclear fuel in power plants. Their main sources are soil, rocks, plants, sand and water. Despite of such benefits, these ions create serious toxicological effects for human since their compounds are potential occupational carcinogens [1, 2]. Nuclear spent fuels generally contain several hazardous metal ions, such as uranium and thorium,

M. S. Hosseini (✉)
Department of Chemistry, Faculty of Science, University of Birjand, Birjand, Iran
e-mail: mshosseini1336@yahoo.com

F. Abedi
Department of Chemistry, Faculty of Science, Islamic Azad University, Neyshabur, Iran

which may be released to environmental media and penetrate into the ground water samples. Previously, liquid–liquid extraction (LLE) as a traditional extraction method was widely used for separation/preconcentration of these metal ions [3–5]. Nowadays, there is a trend to replace the LLE methods with ion exchange and solid phase extraction (SPE) in order to minimize sample manipulation, the metal ions losses and use of toxic solvents. For example, new types of SPE materials, such as highly cross linked polymers and chemically modified polymers, are currently being developed for more effective extraction [6–10]. However, some of the sorbents do co-extract many matrix species resulting to an unclean time-consuming extraction process. Moreover, application of these hybrid materials is uneconomic in industrial scales owing to expensive chemical regeneration, complicated methods of preparation, low capacity, long time-consuming for chemical bonding of chelating agents to the polymeric supports, and instability occurred during their application. Thus, the necessity to develop powerful selective extracting techniques has become an attractive area of research.

Solvent impregnated resins (SIRs) are good alternative to solvent extraction and ion exchange techniques for separation/preconcentration of such metal ions. They combine the advantages of solvent extraction systems including fast mass transfer rates, high distribution and selectivity factors, with the advantages of solid ion exchange techniques such as simplicity of equipment and operation in treatment with very dilute solutions. Moreover, the SIRs can be prepared very easily in comparison with the other extracting methods. To prepare the SIRs, usually, the extractant which dissolved or dispersed in aliquot of an appropriate solvent is subjected to the granular polymeric support according to a simple procedure [11]. Some studies proved that the SIRs containing multifunctional ligands such as Cyanex272 [12], oxine [13], octacarboxymethyl-C-methylcalix[4]resorcinarene [14], Tri-n-dodecylamine [15], eosin [16], and carminic acid [17] are selective organic extractants to produce favorite sorbents for the isolation of uranium and thorium from various analytical matrices. Despite of the favorable merits observed in treatment with these SIRs, their selectivity is almost limited to one of the ions of interest.

One of the significant capabilities of the SIRs is simultaneous impregnation of two ligands on/in the polymeric matrix, which is impossible to prepare similar chemically bonding resins. This future of the SIRs has not been investigated up to now. Recently, we have reported the synthesis of a novel SIR involved mixed-ligands of 1,4-dihydroxyantraquinone (DHAQ) and 1,4-diaminoantraquinon (DAAQ) with 1:1 ratio [18]. This SIR was successfully used for mutual separation/preconcentration of U(VI) and Th(IV) ions. It was observed except that pH of the sample solution, their flow rates mostly influence on such extractions. This exhibition was not observed in treatment with the SIRs prepared in our previous works [19–21]. To clear the role of the mixed-ligands impregnation in the adsorption behavior, preparation and characterization of DAAQ-impregnated resin together with the mixed-ligands SIR containing equal values of DHAQ and DAAQ are the aims of this work. Also, comparison of their behaviors against selective adsorption of Th(IV) and U(VI) ions is proposed using various adsorption equilibrium and kinetic models.

Experimental

Materials and apparatus

All the reagents used were of analytical grade and were supplied by E. Merck, Darmstadt, Germany. Stock solutions of Th(IV) and U(VI) were prepared at concentrations of 1×10^{-3} M by dissolving the appropriate amounts of their nitrate salts in 0.1 M HNO_3. Working solutions from each one of the metal ions were prepared by making appropriate dilutions with distilled water. The following buffered solutions were prepared: hydrochloric acid/potassium chloride (pH 1–2); formic acid/sodium formate (pH 2–4); acetic acid/sodium acetate (pH 4–6); and hydrochloric acid/Tris (hydroxymethylaminomethane) (pH 6–8). The reagent solution of 0.1 % Arsenazo III was made by dissolving 0.025 g of this reagent in 25 mL 0.1 M HNO_3. 1-mL portions of the prepared reagent solution were used for each measurement.

A Corning 130 model pH-meter was utilized for pH measurement. A BKS 305-010, UK Gallencamp automatic shaker was used for shaking the mixtures. A 1601PC Shimadzu UV- spectrophotometer was used for all absorbance measurements with one pair of 10 mm quartz cells. The scanning electron microscopic (SEM) micrographs were obtained using a VEGA//TESCAN instrument at an accelerating voltage of 20 kV.

Preparation of the SIRs

Equal portions (1.5 g) of DAAQ and DHAQ were added to a 50 mL stoppered flask containing 30 mL of dichloromethane. The flask was shaken for a few minutes and then 1.2 g of the cleaned and dried Amberlite XAD-16 was added to the mixture. The shaking was followed for 24 h. After that, the impregnated resin beads were separated using a porous filter, rinsed with 0.1 M HCl until the filtrate solution didn't show any absorbance relevant to the ligands. Then, the impregnated resin was dried at 40 °C for 2 h. The amount of the ligands taken up by the resin was determined by measuring the increase in the weight of the resin after the equilibration followed by the washing and drying processes (impregnation percentage: 57.95).

To prepare the conventional SIR containing DAAQ, this procedure was similarly repeated with only a difference in which 3 g DAAQ was subjected to the impregnation process (impregnation percentage: 34.84).

Adsorption equilibrium procedure

The adsorption isotherms of Th(IV) and U(VI) ions on both types of the SIRs were obtained using the batch technique at the optimum pH values (5 and 6.50 for Th(IV) and U(VI), respectively) and room temperature (298 ± 2 K). For this purpose, several buffered solutions containing Th(IV) or U(VI) with equal volumes (100 mL) and different concentrations involved in the dynamic ranges were placed in conical flasks and 0.07 g of the SIRs was added to each one. The mixtures were shaken for 30 min. Then, aliquots of 5-mL of the supernatants were withdrawn and subjected to the determination process of Th(IV) or U(VI) as discussed in the following.

Adsorption rate procedure

To obtain adsorption kinetic data, a series of fixed weighed portions (0.100 g) of the SIRs were immersed into the vessels containing 100 mL buffered solutions (pH 5.0 for Th(IV) and 6.5 for U(VI)) with concentration of 0.8, 3.8 and 23 mg L^{-1} at room temperature. The mixtures were stirred mechanically for a pre-determined time intervals at a fixed speed (220 rpm). During the stirring of the solutions, portions of 4-mL of the supernatant were withdrawn and subjected to the determination processes indicating the decrease of the metal ions concentrations.

The determinations procedure

The samples obtained from both types of the investigations which contain either Th(IV) or U(VI) ions were transferred to 10 mL volumetric flasks. After addition of 2 mL 37 % HCl and 1 mL 0.1 % Arsenazo III to the flasks, they were diluted to the mark with distilled water. The flasks were shaken for 20 min and absorbance of the solutions were then measured at 659 nm for Th(IV) or 653 nm for U(VI) determinations against the reagent blanks prepared by the same manner.

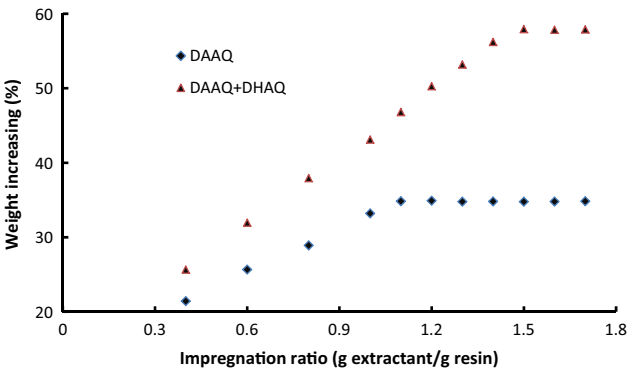

Fig. 1 Effect of impregnation ratio on the weight increasing of both types SIRs

Results and discussion

Characterization of the prepared SIRs

Amberlite XAD-16 is an adsorbent based on polystyrene divinylbenzene copolymer. It has excellent physical

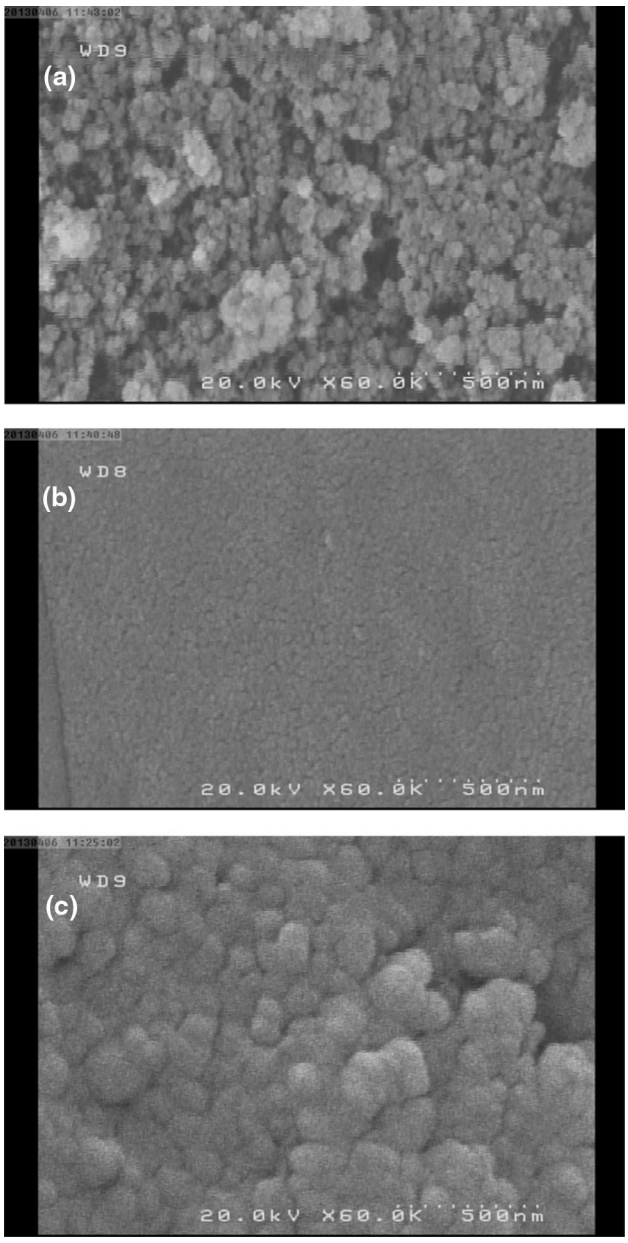

Fig. 2 SEM micrographs of polymeric support samples, **a** Amberlite XAD-16, **b** conventional SIR containing DAAQ, **c** mixed-ligands SIR containing DAAQ + DHAQ

resistance, hydraulic characteristic and thermal stability. Among the XAD series of Amberlite resins which have low polarity, it also benefits from the highest porosity and the largest surface area (825 m^2 g^{-1}). Hence, this type of copolymer was chosen for preparation of the proposed SIRs. The impregnation process to prepare DAAQ-impregnated resin and mixed-ligands-impregnated resin containing DAAQ and AHAQ was carried out at the various impregnation ratios (g ligand/g dry polymer). Figure 1 depicts the weight increase against the impregnation ratio. As it is shown, the diagrams reach to plateau at impregnation ratios more than 1.1 and 1.5 g in treatment with DAAQ and DAAQ + DHAQ per g Amberlite XAD-16, respectively. This observation may be due to the repulsion between the DAAQ molecules in the impregnated phase, which decreases in the presence of DHAQ molecules owing to presence of amine groups. Figure 2 shows the surface morphology of XAD-16 resin beads before and after the impregnation with DAAQ and mixed-ligands of DAAQ + DHAQ. The SEM images clearly show the difference between the surfaces of the SIRs. Although a good uniformity observed in the conventional SIR containing DAAQ but the impregnated layer is more developed in the mixed-ligands SIR. To determine the amounts of DAAQ or DHAQ impregnated on/in the SIRs, they were removed from the resin beads by washing with 4 M H_2SO_4 and measuring their absorbance at the relevant λ_{max} values. The results obtained showed that both the antraquinones were equally impregnated on/in the resin beads.

Effect of pH on the adsorption process

The effect of pH on adsorption behavior of the mixed-ligands SIR was previously investigated [18]. Figure 3 shows the influence of pH in adsorption process of the metal ions onto both types of the SIRs. The data reveals maximum adsorption of Th(IV) and U(VI) ions occur respectively around pH 5 and 6.5, regardless of type the SIRs used.

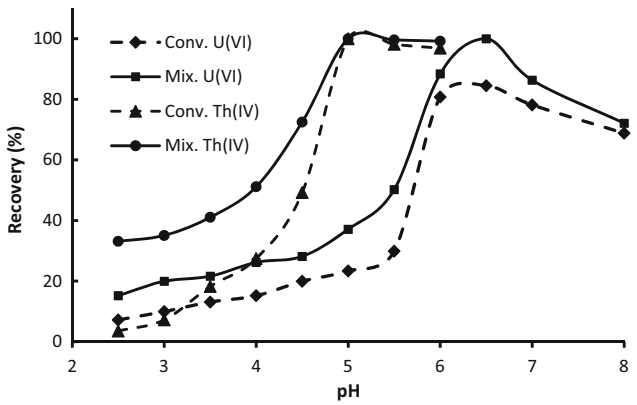

Fig. 3 Effect of pH on adsorption of Th(IV) and U (VI) on/in both types of the SIRs. Aliquots of 100-mL of the solutions containing 0.8 mg L^{-1} Th(IV) or U(VI) were subjected to the prepared SIRs (0.7 g) and shaken for 30 min

Adsorption equilibrium study

Adsorption equilibrium is an important physicochemical feature for the evaluation of the adsorption capacity and adsorption energy of an adsorbent. Expression of adsorption equilibrium is generally carried out via the adsorption isotherm that correlates the amount of solute adsorbed per unit weight of the adsorbent and the concentration of a

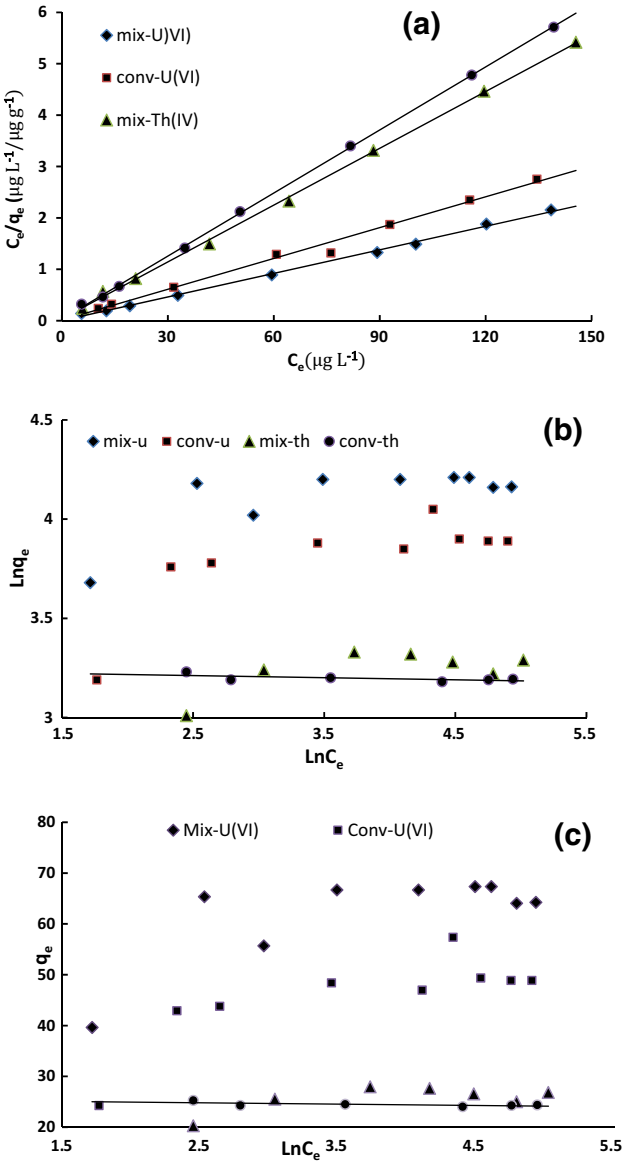

Fig. 4 Linearized forms of adsorption isotherms for adsorption of Th(IV) and U(VI) on/in both types of the SIRs, **a** Langmuir, **b** Freundlich, **c** Temkin

Table 1 Isotherm parameters and equations from Fig. 3 for both types of the SIRs

Langmuir isotherm	Equation	R^2	q_{max}(μg g^{-1})	b (L μg^{-1})
Th(IV)-Con. SIR	$y = 0.0409x + 0.0278$	0.9997	24.450	1.471
Th(IV)-Mix. SIR	$y = 0.0368x + 0.0383$	0.9990	27.174	0.961
U(VI)-Con. SIR	$y = 0.0200x + 0.0113$	0.9907	50.000	1.770
U(VI)-Mix. SIR	$y = 0.0153x + 0.0019$	0.9978	65.360	8.053
Frendlich isotherm	**Equation**	R^2	K_F ($\mu g^{1-(1/n)}$ $L^{1/n} g^{-1}$)	n(g L^{-1})
Th(IV)-Con. SIR	$y = -0.0107x + 3.2381$	0.4195	25.485	15.385
Th(IV)-Mix. SIR	$y = 0.0754x + 2.9433$	0.4195	18.978	16.129
U(VI)-Con. SIR	$y = 0.1607x + 3.2132$	0.5787	24.859	17.580
U(VI)-Mix. SIR	$y = 0.1121x + 3.6951$	0.5347	40.250	34.483
Temkin Isotherm	**Equation**	R^2	B_T (L g^{-1})	A_T(m mol L^{-1})
Th(IV)-Con. SIR	$y = -0.2655x + 25.482$	0.4243	0.006	6.566E7
Th(IV)-Mix. SIR	$y = 1.7553x + 18.756$	0.4018	0.006	3.476E8
U(VI)-Con. SIR	$y = 6.1183x + 23.378$	0.6089	0.002	3.036E43
U(VI)-Mix. SIR	$y = 5.8980x + 39.885$	0.5352	0.008	1.328E16

solute in bulk solution at a given temperature under equilibrium conditions [22]. The Longmuir, Frendlich and Temkin isotherms are of the most widely used isotherm models that have been used for the study of metal ions adsorption onto solid adsorbents. The linear form of these three isotherms can be written according to the following equations:

Langmuir isotherm:

$$\frac{C_e}{q_e} = \frac{1}{q_{max} b} + \frac{C_e}{q_{max}} \quad (1)$$

Frendlich isotherm:

$$\ln q_e = \ln K_F + \frac{\ln C_e}{n} \quad (2)$$

Temkin isotherms:

$$q_e = B_T \ln A_T + B_T \ln C_e \quad (3)$$

It is well-known that the Langmuir equation is applicable to homogeneous adsorption, where the adsorption of each adsorbate onto the surface had equal adsorption activation energy [23]. The Freundlich equation is an empirical expression employed to describe a heterogeneous system [24]. The Temkin isotherm equation assumes that the adsorption of adsorbate is uniformly distributed so that the fall in the heat of adsorption is linear rather than logarithmic. Indeed, with the coverage of surface by the adsorbates, the heat of their adsorption on the layer decreases linearly due to the adsorbate–adsorbate repulsions [25]. In this work, equilibrium studies were performed to identify the best fit isotherm model for explaining the adsorption of Th(IV) and U(VI) onto the prepared SIRs. For this purpose, portions of 0.05-g of both types of the SIRs were kept in contact with aliquots of 100-mL of solutions containing Th(IV) or U(VI) over the concentration ranges of 2–150 m L^{-1}. To attain the maximum adsorption value, pH of the solutions was adjusted to the optimum value using the adequate buffering system while temperature of the solutions was fixed at 298 ± 2 K. The equilibrium data were analyzed using the above triple models by least-squares fit of the adsorption data (Fig. 4). Metal adsorption constants and correlation coefficients for metal ions of interest onto each type of the SIRs are given in Table 1. By comparison the linearity and correlation coefficient obtained in the above models, it was found that the Langmuir isotherm is better describing adsorptions of the metal ions. Conformity of the experimental data to linear plot of Langmuir's model also indicates homogenous distribution of metal ions extracted on the polymeric surface of the resin beads and formation of monolayer coverage the surface of the SIRs during the sorption process. As detailed in Table 1, the monolayer saturation capacities (q_{max}) of the mixed-ligands SIR are greater than the conventional one, regardless of type the metal ion. Moreover, q_{max} value obtained for U(VI) is much greater than Th(IV) in treatment with the mixed-ligands SIR. The relatively high values of adsorption energy (b) of U(VI) ions have been arisen from more strongly chemisorptions of U(VI) than Th(IV) ions on/in the SIRs. Considering the presence of intra-molecular hydrogen bonds in DAAQ and DHAQ, the metal ion adsorption on/in the SIRs can be described by the complex formation between the metal ions

and the ligands through the replacement of this hydrogen atoms with the metal ion. This phenomenon can be indicated as follows:

$$\overline{(QH_2)_n} + UO_2^{2+} \rightleftarrows \overline{(QH_2)_{n-2}UO_2(QH)_2} + 2H^+ \quad (4)$$

$$\overline{(QH_2)_n} + Th^{4+} \rightleftarrows \overline{(QH_2)_{n-2}Th(QH)_2(OH)_2} + 2H^+ \quad (5)$$

where QH_2 represents the antraquinones compounds and the bar denotes the species in the organic phase of the impregnated resin. Mechanism of U(VI) and Th(IV) adsorption on/in the SIR can be discussed by Hall and co-workers showed that the essential characteristics of Langmuir's adsorption isotherm equation could be expressed in terms of a dimensionless constant called as separation factor or equilibrium parameter, (R_L) defined by the Eq. (4) [26].

$$R_L = \frac{1}{1 + bC_O} \quad (6)$$

The value of R_L indicates the nature of the isotherm to be irreversible $(R_L = 0)$, favorable $(0 < R_L < 1)$ and unfavorable $(R_L = 1)$. From the experimental data, the values of R_L were found to be between 0 and 1 for both the metal ions at the initial concentrations, which confirms obeying the Langmuir's model under the operation conditions.

Adsorption kinetics study

The chemical kinetic describes reaction pathways, along times to reach the equilibrium whereas chemical equilibrium gives no information about pathways and reaction rates. Adsorption kinetics show large dependence on the physical and/or chemical characteristics of the adsorbent material, and adsorbate species which also influence the adsorption mechanism. The kinetic transfer of adsorbate species from solution phase to the solid surface of adsorbent particles is often controlled by chemical reaction, film or boundary layer diffusion, diffusion of the adsorbate within the pores of the adsorbent (particle diffusion), pore surface diffusion, and adsorption on the surface [27]. To perform such investigations, several kinetic models, such as the pseudo-first-order and pseudo-second-order adsorption, Elovich, and intraparticle diffusion models were used to describe the adsorption kinetics data. The pseudo-first-order expression of Lagergren [28] is given as

$$\log(q_e - q_t) = \log q_e - \frac{k_1}{2.303} t \quad (7)$$

If the adsorption follows the pseudo-first-order rate equation, a plot of $\log(q_e - q_t)$ against contact time 't' must be a straight line. The pseudo-second-order rate model [29] is expressed as

$$\frac{t}{q_t} = \frac{1}{k_2 q_e^2} + \frac{1}{q_e} t \quad (8)$$

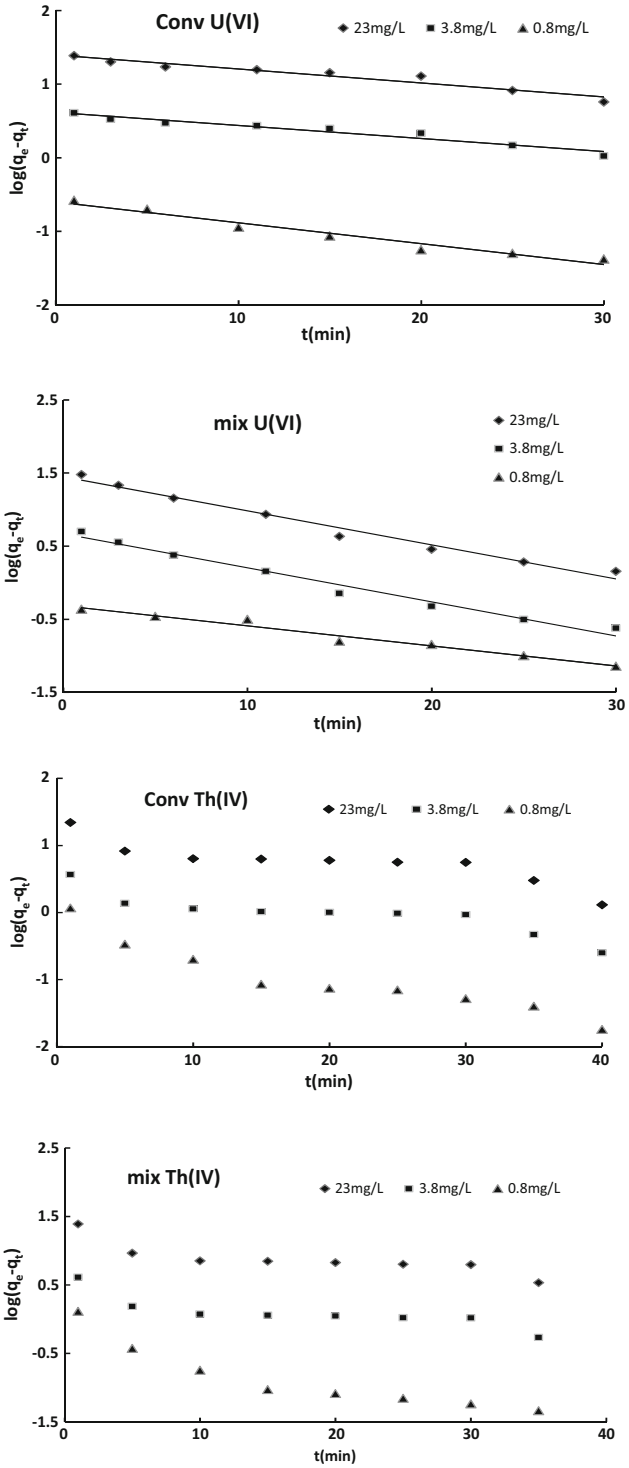

Fig. 5 Plots of adsorption kinetic based on the pseudo first-order equation in treatment with both type of the SIRs

Based on the Eq. 8, the experimental data of q_t, q_e and k_2 can be determined from the slope and the intercept of the plot of t/q_t against t. When the diffusion (internal surface and pore diffusion) of adsorbate species inside the adsorbent is the rate-limiting step, then adsorption data can be

Table 2 Summary of Th(IV) and U(VI) adsorption data evaluated by Pseudo-first-order kinetic model

Metal ion-SIR system	Metal ion concentration (mg/L)	Equation	r^2	q_e (calculated)	Rate constant
Th(IV)-con	23	$y = -0.0214x + 1.1777$	0.7783		
	3.8	$y = -0.021x + 0.3997$	0.7994		
	0.8	$y = -0.0379x - 0.2253$	0.8933		
Th(IV)-mix	23	$y = -0.0168x + 1.1707$	0.7029		
	3.8	$y = -0.0171x + 0.3936$	0.7045		
	0.8	$y = -0.0372x - 0.2073$	0.8331		
U(VI)-con	23	$y = -0.0189x + 1.3935$	0.9350	24.75	0.04353
	3.8	$y = -0.0178x + 0.6148$	0.9460	4.12	0.04099
	0.8	$y = -0.0284x - 0.6006$	0.9610	0.25	0.06540
U(VI)-mix	23	$y = -0.0485x + 1.4896$	0.9772	30.87	0.1117
	3.8	$y = -0.0486x + 0.7119$	0.9773	5.15	0.1119
	0.8	$y = -0.0274x - 0.3168$	0.9731	0.48	0.0631

Table 3 Summary of Th(IV) and U(VI) adsorption data evaluated by Pseudo-second-order kinetic model

Metal ion-SIR system	Metal ion concentration (mg/L)	Equation	r^2	q_e (calculated)	Rate constant
Th(IV)-con	23	$y = 0.0474x + 0.2248$	0.9481	21.10	9,99
	3.8	$y = 0.2833x + 1.4034$	0.9588	3.53	0.06
	0.8	$y = 0.8283x + 1.8193$	0.9995	1.21	0.38
Th(IV)-mix	23	$y = 0.0443x + 0.1779$	0.9738	22.57	0.01
	3.8	$y = 0.2434x + 1.385$	0.9858	4.11	0.04
	0.8	$y = 0.7407x + 1.6299$	0.9990	1.35	0.34
U(VI)-con	23	$y = 0.0318x + 0.7291$	0.8774		
	3.8	$y = 0.2315x + 3.638$	0.8253		
	0.8	$y = 1.9989x + 87.815$	0.5182		
U(VI)-mix	23	$y = 0.0229x + 0.0879$	0.9985	43.67	0.006
	3.8	$y = 0.1375x + 0.5229$	0.9984	7.27	0.036
	0.8	$y = 1.894x + 40.062$	0.9468	0.53	0.090

presented by the following equation, which is known as the simplified Elovich equation [30]:

$$q_t = \frac{1}{\beta}\ln(\alpha\beta) + \frac{1}{\beta}\ln t \quad (9)$$

The intraparticle diffusion [31] equation can be described as

$$q_t = k_i t^{0.5} + I \quad (10)$$

k_i can be determined by the slope of the straight-line portion of a plot of q_t versus $t^{0.5}$. Values of I give an idea about the thickness of the boundary layer. If the adsorption processes conform to intraparticle diffusion, the plot of the uptake (q_t) versus square root of time would result in a linear relationship and the intraparticle diffusion would be the controlling step, providing this line passed through the origin. When the plots do not pass through the origin, this is indicative of some degree of boundary layer control. This future shows that the other processes may associate with intraparticle diffusion at the rate controlling step. Minimum intercept means that adsorption is less boundary layer controlled.

The validity of pseudo first-order and second-order models are usually confirmed by checking the adsorption capacity after finding a linear relationship with considerably high correlation coefficient over the "whole" range of the studies. Conformity the results to pseudo first order or second order equation models denotes the rate is controlled with diffusion or chemisorption process, respectively [31]. Figure 5 shows plots of linearized form of pseudo first order equation for Th(IV) and U(VI) ions adsorption at all concentration studied. The values of q_e and k_1, and the correlation coefficients (r^2) are presented in Table 2. As observed in Fig. 5, the plots of $\log(q_e - q_t)$ against t are linear only for U(VI) adsorption at all the metal ion concentrations, suggesting the process of U(VI) adsorption follows first-order kinetics and it is diffusion-controlled. The r^2 values for these plots are in the range 0.9350–0.9773 and the calculated q_e values obtained from this equation give relatively reasonable values, which are

comparable with experimental q_e values (Table 2). Furthermore, in treatment with the mixed-ligands SIR, the rate constant and calculated q_e values obtained from the higher concentrations of U(VI) are considerably greater than the conventional SIR. Regarding the results observed in Table 2 and SEM images which denotes on higher porosity of mixed-ligands SIR, it may be concluded that adsorption of U(VI) through the diffusion on/in the mixed-ligands SIR is easier than the conventional SIR.

The parameters obtained for the pseudo second-order equation are presented in Table 3. As depicted in Fig. 6, the curve-fitting plots of t/q_t versus t give straight lines for Th(IV) in treatment with both types of the SIRs; although the mixed-ligands SIR exhibits more compatible behavior in comparison with the conventional one. The plots of t/q_t versus t do not show good results for U(VI) during the entire adsorption period, confirming no applicability of the pseudo second-order equation. As detailed in Table 3, in treatment with the mixed-ligands SIR, the r^2 values for this kinetic model are relatively high; however, the calculated q_e values are considerably greater than the experimental values, indicating U(VI) adsorption does not obey from the second-order model at all concentrations.

With regards to adsorption of U(VI) and Th(IV) are in accordance with respectively pseudo first and second order

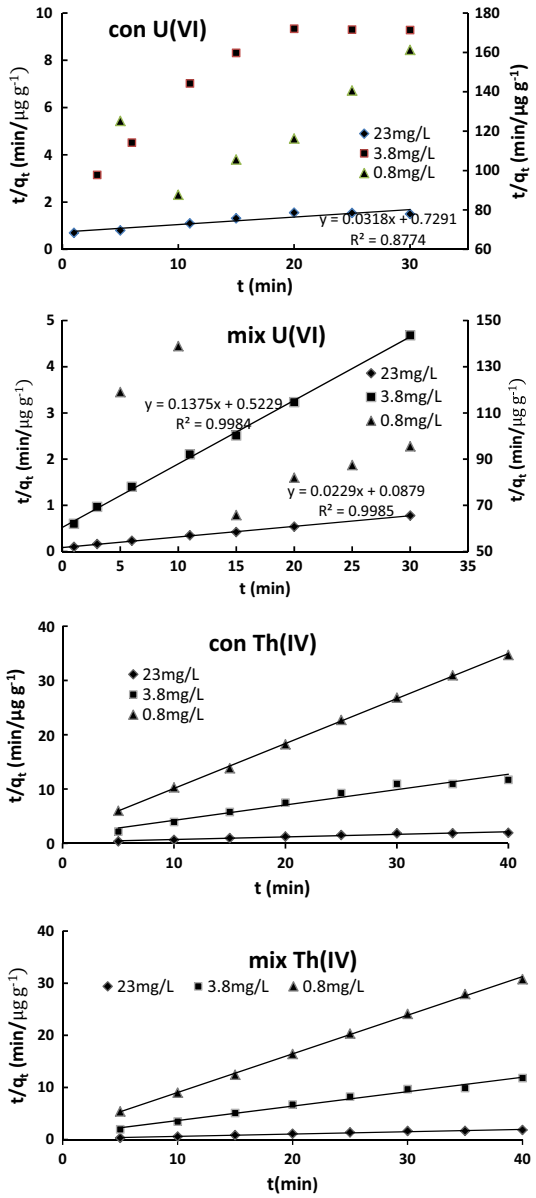

Fig. 6 Plots of adsorption kinetic based on the pseudo second-order equation in treatment with both type of the SIRs

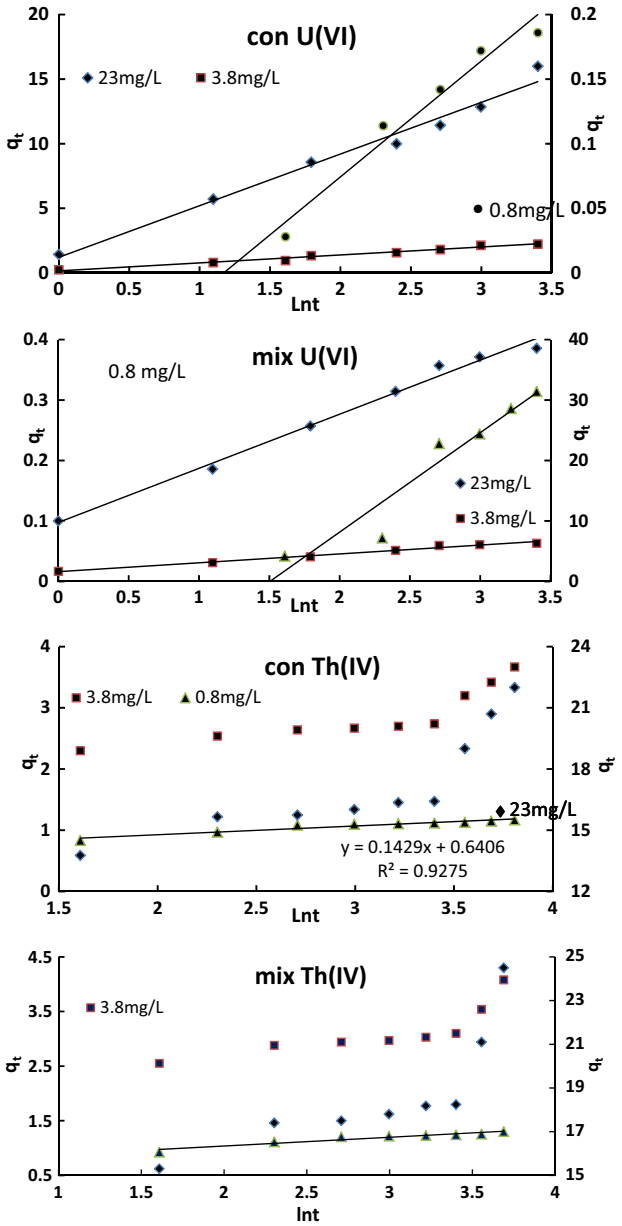

Fig. 7 Plots of adsorption kinetic based on the Elovich equation in treatment with both type of the SIRs

Table 4 Summary of Th(IV) and U(VI) adsorption data evaluated by Elovich kinetic model

Metal ion-SIR system	Metal ion concentration (mg/L)	Equation	r^2	q_e (calculated)	Rate constant
Th(IV)-con	23	$y = 3.1481x + 7.753$	0.7149		
	3.8	$y = 0.5333x + 1.2587$	0.7251		
	0.8	$y = 0.1429x + 0.6406$	0.9275	6.9979	1,327
Th(IV)-mix	23	$y = 3.1893x + 9.3919$	0.6364		
	3.8	$y = 0.5452x + 1.5359$	0.6679		
	0.8	$y = 0.1604x + 0.7152$	0.9171	6.2344	1,296
U(VI)-con	23	$y = 3.9976x + 1.2064$	0.9809	0.2502	20.28
	3.8	$y = 0.6159x + 0.1509$	0.9775	1.6236	19.16
	0.8	$y = 0.0897x - 0.1051$	0.9640	11.15	4.65
U(VI)-mix	23	$y = 8.951x + 9.7519$	0.9897	0.11	44.59
	3.8	$y = 1.466x + 1.6061$	0.9858	0.68	44.86
	0.8	$y = 0.1645x - 0.2474$	0.9215	6.08	3.33

models, their adsorption occur probably via surface exchange reactions until the surface functional sites are fully occupied; thereafter, the metal ions diffuse into the SIR for further ion-exchange reactions [32]. This mechanism may be partly due to complexation between the negatively charged groups of ligands and the positively charged metal ions.

Figure 7 shows plots of the Elovich equation for the same experimental data in which significant linearity is observed between adsorbed values of U(VI), q_t, and ln t throughout the adsorption period in treatment with both types of the SIRs. The relevant correlation coefficients were obtained between 0.9215 and 0.9897 for all of the linear plots (Table 4). The Elovich equation does not predict any definite mechanism; however, it is useful for describing adsorption on highly heterogeneous adsorbents such as the mixed-ligands SIR. In this situation, the Elovich equation can be used to predict the adsorption kinetics of U(VI) as a borderline hard acid on/in the SIRs, especially in treatment with the mixed-ligands SIR due to presence of more active heterogeneous surface with higher basicity in comparison with the other one. In the case of using the Elovich equation for Th(IV) ions adsorption, linear relationships are observed between Th(IV) adsorbed, q_t, and ln t at the initial adsorption period (Fig. 7). Considering the whole Th(IV) adsorption period, the correlation coefficients are lower than those of U(VI) adsorption owing to presence of N-donor groups in both types of the SIRs. Hence, Th(IV) as a strong hard acid exhibits more tendency to react with the functionalized surface of the SIRs.

Figure 8 represents the plot of q_t versus $t^{0.5}$ for the same experimental data. At first glance, nonlinearity observed for all of the concentrations; however, precise observation shows that the data points can be better represented by two or three straight lines with difference in slope (k_i) and

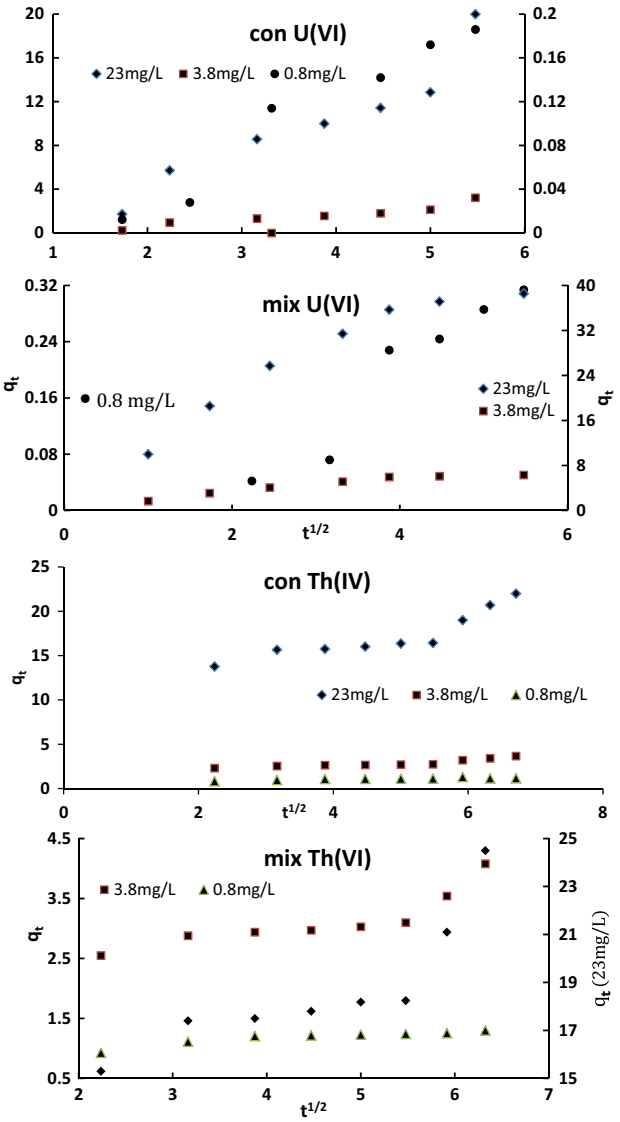

Fig. 8 Plots of adsorption kinetic based on the Intraparticle diffusion equation in treatment with both type of the SIRs

Table 5 Summary of Th(IV) and U(VI) adsorption data evaluated by intraparticle diffusion kinetic model

Metal ion-SIR system	Metal ion concentration (mg/L)	Equation	r^2	q_e (calculated)	Rate constant
Th(IV)-con	23	$y = 1.6093x + 9.5787$	0.8092		
	3.8	$y = 0.2728x + 1.567$	0.8220		
	0.8	$y = 0.0759x + 0.7276$	0.7608		
Th(IV)-mix	23	$y = 1.6974x + 11.016$	0.7193		
	3.8	$y = 0.2896x + 1.8164$	0.7518		
	0.8	$y = 0.0763x + 0.838$	0.8289		
U(VI)-con	23	$y = 3.8958x - 4.4046$	0.8989		
	3.8	$y = 0.6783x - 1.0742$	0.7200		
	0.8	$y = 0.0485x - 0.0722$	0.9609		0.0485
U(VI)-mix	23	$y = 6.5039x + 7.4169$	0.9168		6.5039
	3.8	$y = 1.0681x + 1.2149$	0.9179		1.0681
	0.8	$y = 0.09302x - 0.1699$	0.9302		0.0930

intercept (I). The values of k_i and I are summarized in Table 5 along with regression constant (r^2) at different initial concentrations of metal ions. In the first straight line, the sudden increase (within a short period of time) in slope signifies that the metal ions are transported to the external surface of the SIRs through film diffusion therefore the adsorption rate is very fast. After that, the metal ions enter into the resin particles by intra-particle diffusion through pores, which is represented in second straight line. In any case, the line does not pass through the origin since both film diffusion and intraparticle-diffusion are simultaneously occurring during the adsorption of metal ions of interest on/in the SIRs and the intraparticle diffusion is not the only rate controlling step. In addition, the performance of the mixed-ligands SIR is considerably better than the conventional one due to the presence of higher porosity.

Conclusion

Obviously, due to the presence of carbonyl and amine groups in the DAAQ-impregnated resin, it is capable to react with U(VI) and Th(IV) through the complexation process. Contribution of DHAQ in the impregnation process gives rise to enhance selectivity and capacity toward U(VI) ions in comparison with Th(IV) ions during their co-extraction with the mixed-ligands SIR. The following benefits are outlined in comparison between the mixed-ligands SIR and the conventional DAAQ-impregnated resin:

(1) Higher impregnation percentage of the mixed-ligands SIR (57.95) in comparison with the conventional SIR (34.84) indicates higher capacity and extraction ability of the mixed system.
(2) Usually, the SEM micrographs are used to observe surface morphological changes of the adsorbent materials during the preparation process. Figure 2 shows the surface morphology of XAD-16 resin beads before and after the impregnation process. The SEM images clearly show the higher impregnation efficiency of the mixed-ligands SIR.
(3) In treatment with the mixed-ligands SIR, the monolayer saturation capacities (q_{max}) relevant to both metal ions of interest are greater than the conventional one.
(4) As regards the kinetic investigations, it was established that the adsorption behavior of U(VI) ions completely differs from Th(IV) ions in treatment with the mixed-ligands SIR. Compatible with the proposed model in comparison with the conventional one.
(5) The results showed that the mixed-ligands SIR has the sufficient potential for the mutual separation of U(VI) and Th(IV). These observations clarify the results obtained from the successful separation and preconcentration of these metal ions in our earlier report [18].

Acknowledgments The authors wish to thank the University of Birjand and Islamic Azad University-Neyshabur, Iran for their financial support.

References

1. Clayton GD, Clayton FE (eds), (1994) Patty's Industrial Hygiene and Toxicology. 2C 2735
2. Agency for Toxic Substances and Disease Registry (2000) U.S. Public Health Service, Chapman and Hall, New York
3. Condamines N, Musikas C (1992) The extraction by N.N-dialkylamides. II. Extraction of actinide cations. Solvent Extr Ion Exch 10:69–100
4. Mowafy EA, Aly HF (2002) Extraction behaviours of Nd(III), Eu(III), La(III), Am(III), and U(VI) with some substituted malonamides from nitrate medium. Solvent Extr Ion Exch 20:177–194

5. Ardois C, Musikas C, Fattahi M, Abbe AC (1992) Selective actinide solvent extraction used in conjunction with liquid scintillation. J Radioanal Nucl Chem 226:241–245
6. Gupta B, Malik P, Deep A (2002) Extraction of uranium, thorium and lanthanides using Cyanex-923: Their separations and recovery from monazite. J Radioanal Nucl Chem 251:451–456
7. Maheswari MA, Subramanian MS (2004) Selective enrichment of U(VI), Th(IV) and La(III) from high acidic streams using a new chelating ion-exchange polymeric matrix. Talanta 64:202–209
8. Prabhakaran D, Subramanian MS (2005) Selective extraction of U(VI) over Th(IV) from acidic streams using di-bis(2-ethylhexyl) malonamide anchored chloromethylated polymeric matrix. Talanta 65:179–184
9. Prabhakaran D, Subramanian MS (2004) Selective extraction of U(VI), Th(IV), and La(III) from acidic matrix solutions and environmental samples using chemically modified Amberlite XAD-16 resin. Anal Bioanal Chem 379:519–525
10. Jain VK, Pandya RA, Pillai SG, Shrivastav PS (2006) Simultaneous preconcentration of uranium(VI) and thorium(IV) from aqueous solutions using a chelating calix[4]arene anchored chloromethylated polystyrene solid phase. Talanta 70:257–266
11. Kabay N, Gizli N, Demirel N, Demircioglu M, Yuksel M, Saglam M (2003) Removal of cadmium from phosphoric acid solutionby solvent-impregnated resins (sirs) sorption kinetics and equilibria studies. Chem Eng Comm 190:936–947
12. Karve M, Rajgor RV (2008) Amberlite XAD-2 impregnated organophosphinic acid extractant for separation of uranium(VI) from rare earth elements. Desalination 232:191–197
13. Singh BN, Maiti B (2006) Separation and preconcentration of U(VI) on XAD-4 modified with 8-hydroxy quinolone. Talanta 69:303–396
14. Merdivan M, Pirinccioglu N, Hamamci C (2003) Thorium(IV) and uranium(VI) adsorption studies on octacarboxymethyl-C-methylcalix[4] resorcinarene impregnated on a polymeric support. Anal Chim Acta 485:213–219
15. Metwally E, Saleh ASh, El-Naggar HA (2005) Extraction and Separation of Uranium (VI) and Thorium (IV) Using Tri-n-dodecylamine Impregnated Resins. J Radioanal Nucl Chem 6:119–126
16. Hosseini MS, Hosseini-Bandegharaei A (2010) Selective extraction of Th(IV) over U(VI) and other co-existing ions using eosin B-impregnated Amberlite IRA-410 resin beads. J Radioanal Nucl Chem 283:23–30
17. Hosseini-Bandegharaei A, Hosseini MS, Jalalabadi Y et al (2013) A novel extractant-impregnated resin containing carminic acid for selective separation and pre-concentration of uranium(VI) and thorium(IV). Int J Environ Anal Chem 93:108–124
18. Hosseini MS, Abedi F (2014) Stepwise extraction of Th(IV) and U(VI) ions with mixed-ligands impregnated resin containing 1,4-diaminoanthraquinone and 1,4-dihydroxyanthraquinone. J Radioanal Nucl Chem. doi:10.1007/s10967-014-3366-9
19. Hosseini MS, Hosseini M, Hosseini-Bandegharaei A (2007) Solvent impregnated resins containing quinizarin: preparation and application to batch-mode separation of Cd(II), Cu(II), Ni(II), and Zn(II) in aqueous media prior to the determination by flame atomic absorption spectrometry. Sep Sci Technol 42:3465–3480
20. Hosseini MS, Hosseini-Bandegharaei A, Hosseini M (2009) Column-mode separation and pre-concentration of some heavy metal ions by solvent-impregnated resins containing quinizarin before the determination by flame atomic absorption spectrometry. Int J Environ Anal Chem 89:35–48
21. Hosseini MS, Hosseini-Bandegharaei A (2011) Comparison of adsorption behavior of Th(IV) and U(VI) on modified impregnated resin containing quinizarin with that conventional prepared impregnated resin. J Hazard Mater 190:755–765
22. Aveyard R, Haydon DA (1973) An Introduction to the Principles of Surface Chemistry. Cambridge University Press, Cambridge, p 201
23. Langmuir I (1916) The constitution and fundamental properties of solids and liquids. J Am Chem Soc 38:2221–2295
24. Freundlich H (1906) Adsorption in solution. Phys Chem Soc 40:1361–1368
25. Ozacar M, Sengil IA (2005) Adsorption of metal complex dyes from aqueous solutions by pine sawdust. Bioresour Technol 96:791–795
26. Hall KR, Eagleton LC, Acrivos A, Vermeulen T (1966) Pore and solid diffusion kinetics in fixed-bed adsorption under constant pattern conditions. Ind Eng Chem Fundam 5:212–223
27. Bulut E, Ozacar M, Sengil IA (2008) Equilibrium and kinetic data and process design for adsorption of Congo red onto bentonite. J Hazard Mater 154:613–622
28. Mane VS, Mall ID, Srivastava VC (2007) Use of bagasse fly ash as an adsorbent for the removal of brilliant green dye from aqueous solution. Dyes Pigments 73:269–278
29. McKay G, Ho YS (1999) Pseudo-second-order model for adsorption processes. Process Biochem 34:451–465
30. Chein SH, Clayton WR (1980) Application of Elovich equation to the biomass of phosphate release and adsorption on soil. Soil Sci Soc Am J 44:265–268
31. Weber WJ, Morris JC, Sanit J (1963) Kinetics of adsorption on carbon from solution. Eng Div Am Soc Civil Eng 89:31–60
32. Ho Y-S (2004) Citiation review of Lagergren kinetic rate equation on adsorption reactions. Scientometrics 59: 171–177